

1           **Illuminating snow droughts: The future of Western  
2           United States snowpack in a high-resolution coupled  
3           global climate model**

4           **Julian Schmitt<sup>1</sup>, Kai-Chih Tseng<sup>23</sup>, Mimi Hughes<sup>4</sup>, Nathaniel Johnson<sup>2</sup>**

5           <sup>1</sup>Harvard University

6           <sup>2</sup>Geophysical Fluid Dynamics Laboratory

7           <sup>3</sup>Princeton University

8           <sup>4</sup>Earth System Research Laboratories/ Physical Sciences Laboratory

9           **Key Points:**

- 10          • Driven largely by last two decades, western U.S. severe snow droughts have increased  
11           in frequency by 40-50% across all major watersheds over the last 60 years.
- 12          • The SPEAR climate model accurately simulates the rapid acceleration of west-  
13           ern U.S. severe snow drought that began in the early 2000s.
- 14          • SPEAR projects that increasing temperatures will cause the West to transition  
15           to a low or no-snow environment by the end of the 21st century.

**Abstract**

Seasonal snowpack in the Western United States (WUS) is crucial for meeting summer hydrological demands, reducing the intensity and frequency of wildfires, and supporting snow-tourism economies. While the frequency and severity of snow drought is expected to increase under continued global warming, quantifying both the response of snow drought to radiative forcing and uncertainties owing to internal climate variability provides a significant challenge. To evaluate the projected changes in WUS snow droughts and the uncertainties tied to internal climate variability, we analyzed a 30-member large ensemble of a global climate model with moderately high atmospheric resolution ( $\sim 50\text{km}$ ), the Seamless System for Prediction and EArth System Research (SPEAR). To monitor changes in WUS snow droughts in both observations and SPEAR, we developed a non-parametric drought classification scheme for monthly snowpack. We find that SPEAR projects dramatic increases in snow droughts, with a 8.8-fold increase in snow drought occurrence under SSP5-8.5 and a 5.2-fold increase under SSP2-4.5 emissions pathways by 2100 averaged over the ensemble. We found these changes to be primarily driven by an increase in average monthly temperature anomalies. When tracking the transition to no-snow conditions, defined as over 90% of a watershed's historically snowy region's April snowpack being less than 10% of its historical April average, we found large variability in onset times attributable to internal climate variability. Across the SSP5-8.5 30-member ensemble spread, SPEAR projects that California, for example, could experience no-snow conditions as early as 2058 or as late as 2096. This wide range emphasizes the large irreducible uncertainty of internal climate variability on WUS snow drought changes that has large implications for water management and habitability over the coming century.

**Plain Language Summary**

When winter snow on the ground is significantly less than normal, a region is said to experience a snow drought. Recently, the Western United States has seen a sharp uptick in the frequency of severe snow droughts. Since the region depends on stored mountain snowpack, the snow droughts have exacerbated water shortages and wildfires. Here, we use a new climate model to examine trends in snow droughts through 2100, finding that under a high emission scenario, they could increase nearly 9 fold in frequency by 2100. Using a large ensemble model, we examine how internal climate variability impacts how quickly regions reach a state of "no-snow" in April. California, for example, reaches no-snow conditions anywhere from 2058 to 2096 under the high emissions scenario.

**1 Introduction**

Mountains in the Western United States (WUS) have been coined the "water towers" of the West, storing winter precipitation as snow and releasing it during the dry spring and summer as meltwater to populations which have high, and ever-increasing water needs (Barnett et al., 2005). Alongside direct benefits of sustained snowpack to human irrigation and water needs, several indirect benefits such as reduced forest fires (Trujillo et al., n.d.; Gergel et al., n.d.) and improved snow tourism economics, makes snowpack essential to the WUS' environment and its people. Low or variable snowpack means the opposite: decreased water security, increased fire season activity, and unpredictable snow conditions for tourism (Wobus et al., 2017). Despite large variability from season to season, climate change is already having a measurably significant impact on WUS snowpack, moving towards decreasing snowpack, particularly in late winter (Barnett et al., 2005; Huning & AghaKouchak, 2020). When snowpack, or snow-water equivalent (SWE - the depth of water if all snow melted instantaneously) levels fall significantly below normal, the region is said to experience a snow drought. Snow drought affects the WUS' economy and human activities including areas which rely on streamflow or crop production that are not necessarily covered by winter snowpack.

While hydrological drought has immediate impacts on water resources and availability, the impact of snow droughts (SDs) is typically not felt until summer when early or low snowmelt can exacerbate meteorological drought. Mountains also play a key role in the WUS water supply, as their lower temperatures and higher precipitation capture significant reserves in snow pack. The WUS dry summers makes it reliant on a steady supply of melting water throughout much of the summer and winters with low snowpack typically exacerbating water shortages and wild fires (Barnett et al., 2005; Trujillo et al., n.d.; Gergel et al., n.d.). The type of snow drought also has significant impact on the effects. Dry snow droughts occur when a lack of precipitation results in low stream flow during the melt season, while a warm snow drought is characterized by rapid early season snowmelt resulting in increased reservoir flood risk in early spring, followed by drought conditions as mountain snow is quickly depleted (Harpold et al., 2017). Shrestha et al. (2021) have shown that there is a critical threshold of -6 to -5°C for average winter temperatures above which additional warming begins to significantly decrease snowpack. The WUS falls into this category and therefore its snowpack is vulnerable to any level of warming (Shrestha et al., 2021).

Previous literature has shown that there remains large observational uncertainty in climatological SWE across the WUS, primarily due to low sampling and trouble resolving mountain snowpack in VIC and large-ensemble coupled global climate models (McCrory et al., 2017; Kim et al., 2021; Wrzesien et al., 2019; McCrary et al., 2022). Despite large biases and variability in simulating climatological SWE, these models exhibit robust decreases in WUS SWE (Matiu & Hanzer, 2022). We use a 30-member initial condition state-of-the-art coupled large ensemble global climate model, called the Seamless System for Prediction and EArth System Research Large Ensemble (hereafter SPEAR) to focus on changes in snow drought frequency and intensity as compared with the historical period. Huning and AghaKouchak (2020) has shown that SD total duration, average duration, and intensity in the WUS has increased by 28% between 1980 and 2018, while Shrestha et al. (2021) finds that conditions are expected to continue to worsen because of the WUS' low latitude. We focus on quantifying the uncertainty of these trends that is attributable to both internal climate variability and emissions uncertainty. Specifically, we assess the spread of severe snow drought (D2+ SD) frequency, the variability in average drought/non-drought conditions, and the distribution of the timing to a no-snow regime by WUS watershed region. We look to both verify the SPEAR ensemble simulations by looking over the historical period (1921-2014) with observed time-varying natural and anthropogenic radiative forcing, and to future projections (2014-2100) under a "middle of the road" (SSP2-4.5) and a high emissions scenario (SSP5-8.5) (Delworth et al., 2020). The 30 ensemble runs for each future scenario and two concentration pathways allow us to explore variability across not only the emissions scenarios but also within the ensemble under identical emissions to estimate the internal climate variability.

We first show that SPEAR simulates WUS snow drought changes across the historical period (1921-2011) that are consistent with those of an observational dataset and with previous studies (Huning & AghaKouchak, 2020). We then explore the magnitude of the projected changes by assessing the proportion of months that experience D2+ SD, looking both at the ensemble mean spatio-temporally and the ensemble spread through time. To investigate what is driving the rapid acceleration in D2+ SD frequency, we decompose drought conditions by temperature and precipitation deviation to assess how the conditions under which snow droughts occur changes through time. We then provide a watershed-level assessment of the risk of becoming "snow-free" by the end of the century that explicitly accounts for both scenario uncertainty and internal climate variability.

116 **2 Data and Methods**117 **2.1 SPEAR Large Ensemble Global Climate Model**

118 To assess historical and future changes in snow drought, we analyzed snow water  
 119 equivalent (SWE) values across the Western United States from the 30-member **S**eamless  
 120 **P**eriodic **E**arth **R**esearch large ensemble (hereafter SPEAR)  
 121 (Delworth et al., 2020). SPEAR is a coupled global climate model recently developed  
 122 at the NOAA Geophysical Fluid Dynamics Laboratory (GFDL) that is designed for im-  
 123 proved prediction on a seasonal to decadal timescales. SPEAR comprises GFDL's AM4  
 124 atmosphere, LM4 land, MOM6 ocean, and SIS2 sea-ice models. These component mod-  
 125 els are the same as GFDL's Global Climate Model version 4 (CM4, Held19), which is  
 126 a contributor to the Coupled Model Intercomparison Project, phase 6 (CMIP6), but SPEAR's  
 127 configuration and physical parameterization choices are optimized for climate prediction  
 128 and projection from seasonal to centennial timescales. SPEAR has moderately high res-  
 129 olution in the atmosphere and land ( 50 km resolution) and a coarser ocean and sea ice  
 130 horizontal resolution of about 1° which telescopes to 0.33° meridional spacing near the  
 131 equator .

132 We specifically use SPEAR's monthly SWE, temperature, and precipitation across  
 133 the historical period, from 1921-2014, as well as projections from 2014-2100 under SSP2-  
 134 4.5 and SSP5-8.5 emissions scenarios.

135 **2.2 Observational Data**

136 To evaluate SPEAR's historical simulation of SWE, temperature, and precipita-  
 137 tion we use an observations-based dataset (Livneh et al., 2013), available from 1915 to  
 138 2011, hereafter the Livneh dataset. Livneh is statistically gridded from in situ observa-  
 139 tions of precipitation and temperature to 1/16° resolution, and contains daily temper-  
 140 ature, precipitation observations, plus SWE estimates which are generated using the VIC  
 141 land model. To compare with the SPEAR ensemble members we re-gridded Livneh to  
 142 SPEAR's 1/2° grid and re-sampled to SPEAR's monthly timescale. Despite incorporat-  
 143 ing observational data, SWE has perennially been hard to constrain (Wrzesien et al., 2019).  
 144 Many recent papers have found SWE estimates to vary widely, upwards of a factor of  
 145 3 in some cases (Wrzesien et al., 2019) leading us to expect significant absolute biases  
 146 between SWE estimates (McCrary et al., 2017, 2022), of which Livneh is only one rep-  
 147 resentation. To overcome this issue, we focus our analysis on proportional changes, com-  
 148 paring SWE values to their own historical distributions within each dataset, and then  
 149 comparing these relative changes across datasets.

150 We chose 1921-2011 as our historical period as it is the overlapping period between  
 151 the Livneh dataset and the historical SPEAR dataset. This provided 90 complete win-  
 152 ters (91 years) which we used to validate SPEAR and to develop a baseline to which we  
 153 compare the modeled future climatology. We chose to consider data at monthly resol-  
 154 ution intervals for three reasons: (1) data availability, as SPEAR only recorded SWE at  
 155 monthly intervals, (2) consistency with previous studies, as other papers have done sim-  
 156 ilar analysis (Huning & AghaKouchak, 2020), and (3) monthly resolution is an appro-  
 157 priate timescale for monitoring snow drought.

158 **2.3 Data Comparison**

159 To validate SPEAR SWE, precipitation, and temperature, we first compare the his-  
 160 torical SPEAR runs to the Livneh dataset over the historical period. Livneh contains  
 161 a single realization of the historical period, e.g. what actually happened, while the SPEAR  
 162 ensemble runs capture many possible historical climates. Thus, we do not expect the Livneh  
 163 measurement to align with the SPEAR ensemble mean because changes to the ensem-  
 164 ble mean represent the radiatively forced component of the climate with internal vari-

ability filtered out. The internal variability is an essential component of individual realizations, contributing significantly to inter-model spread in CMIP multi-model ensembles (Deser et al., n.d.). We do expect, however, that SPEAR will simulate a realization of the climate at least as extreme as the observed historical climate over most regions, although with only 30 members it's still reasonable to expect some observations may fall outside of the SPEAR spread. Thus, if we derive similar metrics from both datasets and the observational Livneh realization falls within the SPEAR ensemble spread, then we can assume that SPEAR produces a realistic historical climate. Similarly by comparing changes in the historical period we can assert whether or not SPEAR reasonably captures climate trends.

## 2.4 Drought Classification

Before we can begin to assess changes in snow drought measurements, we must first define snow drought, which is based on the historical distribution of SWE values per month by both grid-cell and region. For subsequent analysis, we restrict our region of study to areas that historically have seasonal snowpack maxima that average above 20mm SWE, based on the SPEAR ensemble mean, we call this the “historically snowy” region. This ensures regions that do not typically have snow are not eligible for classification as snow drought.

Our methodology uses standardized indices which compare a region’s SWE values to its historical climatology, using the US Drought Monitor’s drought classification method for hydrological drought to categorize observations into descriptive bins; near normal, abnormally dry, and moderate, severe, extreme, and exceptional drought, see Figure ?? (Svoboda et al., 2002). Here we use a non-parametric empirical model for SWE, temperature, and precipitation deviations. Without assuming the underlying distributions, a non-parametric model allows us to efficiently capture the variability without imposing subjective constraints on the data and allows us to compare drought frequency and severity across different hydrological regions and different datasets.

We assign each winter month of the year (Oct-April) a score based on the historical conditions at that location. Our time indices are by year and month, e.g.  $t_{1931,1}$  for January 1931, and spatial indices are at intervals of 0.5 degrees of latitude and longitude. Thus  $s_{i,j}^{t_{1931,1}}$  corresponds to a SWE value at latitude-longitude pair  $(i,j)$  during January 1931. We now compute an empirical distribution over  $\mathbf{S}_{i,j}^k = (s_{i,j}^{t_{1921,k}}, s_{i,j}^{t_{1922,k}}, \dots, s_{i,j}^{t_{2011,k}})$ , representing the SWE values during month  $k$  at location  $(i,j)$  over the historical period. We assign z-scores to each location and time stamp using the empirical cumulative distribution function,  $\hat{F}_{i,j}^k$  which assigns each SWE value a number in  $(0, 1)$  based on the proportion of the observed data in  $\mathbf{S}_{i,j}^k$  that fall below it. In equation 1,  $\mathbb{I}$  represents an element-wise indicator for each element of  $\mathbf{S}_{i,j}^k$  being below  $x$  and  $N$  represents the total number of measurements, in this case  $2011 - 1921 = 90$ .

$$\hat{F}_{i,j}^k(x) = \frac{\text{no. of SWE values less than } x}{N_m} = \frac{1}{N_m} \sum_{l=1}^{N_m} \mathbb{I}(\mathbf{S}_{i,j}^k < x) \quad (1)$$

For each observed or simulated SWE value,  $s_{i,j}^{t_{y,k}}$ , we can then compute the z-score by inserting the SWE value into the corresponding  $\hat{F}$  and then into the inverse normal distribution. We refer to these scores as ZSWE, which are index by location, month, and year, and define them as such:

$$ZSWE_{i,j}^{y,m} = \Phi\left(\hat{F}_{i,j}^m(s_{i,j}^{y,m})\right) \quad (2)$$

We classify each month by a drought severity label D0-D4, with NN classifying a month as near normal and W0-W4 increasingly wet months see (supplemental Table ?? for the full classification scheme). While we mostly use this framework to classify snow droughts,

we extend the methodology to temperature and precipitation classification as needed. A similar empirically derived methodology is used by Huning and AghaKouchak (2020) to classify snow droughts across the Alps, Himalayas, and Western United States. More generally, this framework is inspired by the US Drought Monitor which uses the same D0-D4 classification. Their classification scheme, however, is not purely statistical, instead relying on local experts for the final say on the drought classification. As we cannot rely on experts, our model attempts to match the frequency of meteorological droughts in the US Drought Monitor with snow drought frequency. While this may in some locations result in a mismatch of SWE values and impact, it provides a statistical way to capture extremes.

## 2.5 Computing Changes in Snow Drought

We can now apply our drought classification scheme to calculate changes in snow drought across the historical period. We used two 40-year windows, with our early historical period ranging from 1931-1970 and our late historical period from 1971-2011. We aggregate snowpack by HUC2 region, see Figure 1c, and count the total number of occurrences of each extreme event, where we define an extreme event as that which meets a D2+ classification or a z-score of  $< -1.3$ , e.g.  $\mathbb{I}(Z_R^t < -1.3)$  for region  $R$  at time  $t$ . The percent change for a given region,  $\Delta_R$ , is derived via

$$\Delta_R = \frac{\sum_{t'} \mathbb{I}(Z_R^{t'} < -1.3)}{\sum_t \mathbb{I}(Z_R^t < -1.3)} \text{ for } t \in (1930, 1970), t' \in (1971, 2011) \quad (3)$$

For example, the Livneh dataset experienced 27 months of D2+ SD in the early historical period for the Upper Colorado Region, with 28 observations in the late historical period, translating to an increase of 3.7%. We leverage the ensemble spread below to determine whether the overall trend is significant.

## 2.6 Snow Transition Threshold

We are also motivated to determine how a changing snowpack will affect water resources more directly than looking at droughts alone allows. Broadly we want to determine when a shifting climate will begin to severely and persistently impact snow as a water resource. Long-term droughts are particularly damaging, as one or two years of low snow-pack can be buffered by groundwater or above-ground reservoirs. Thus, we are particularly interested in determining when no-snowpack is expected to become systemic (Siirila-Woodburn et al., 2021).

Alongside changes in snow drought characteristics, understanding the fraction of snow that remains in a typical year is important for water management (Harpold et al., 2017). To assess this threat, we calculate the fraction of April SWE that remains in historically snowy regions across each of the 5 HUC2 watersheds. We classify an April ( $m = 4$ ) grid cell  $s_{i,j}^{t,4}$  as no-snow (or snow free) for that year if there is *at most* 10% of the historical snowfall average remaining at the location (Siirila-Woodburn et al., 2021). We then calculate the regional no-snow area proportion as the fraction of the historically snowy region which experiences those conditions. We let  $\mathcal{N}_R^Y$  to denote this no-snow area proportion, where  $R$  represents the region, and  $Y$  the year. As before,  $t_Y \bar{S}_{i,j}^{t_Y,4}$  is the average historical SWE value for the grid cell and  $s_{i,j}^{t_Y,4}$  the SWE value for the specific year. Using 10% as our snow free threshold,  $\mathcal{T} = 0.1$ , then  $\mathcal{N}_R^Y$  can be written as:

$$\mathcal{N}_R^Y = \frac{\sum_{(i,j) \in R} \mathbb{I}(s_{i,j}^{t_Y,4} < \mathcal{T} \cdot \bar{S}_{i,j}^{t_Y,4})}{|(i,j) \in R|} \quad (4)$$

Thus we have a fraction of the historically snowy region that is snow free in a given year in April. To assess when no-snow conditions become endemic, we apply a 10 year moving-

window mean and then define the no-snow transition time as the year when the moving-window mean *last* crosses the area threshold,  $\mathcal{A} = 0.5, 0.75, 0.9$  before 2100. Applying this procedure to all ensemble members, we compute a distribution for when these conditions are likely to become endemic. Formally, the no-snow transition time,  $\mathcal{T}$ , is given by:

$$\mathcal{T} := \left[ \min t : \mathcal{N}_R^{t'} \geq \mathcal{A} \forall t' < t \leq 2100 \right] \quad (5)$$

Where  $\tilde{\mathcal{N}}_R^{t'}$  gives the moving-window mean fraction of region  $R$  that experiences no-snow conditions at time  $t'$ . By requiring the moving-window average to be above  $\mathcal{A}$  for all subsequent years (until 2100),  $\mathcal{T}$  is uniquely determined. For a graphical explanation of this method please refer to supplemental materials' Figure ??.

### 3 Results

#### 3.1 SPEAR Model Evaluation

##### 3.1.1 SPEAR Ensemble Mean Bias

We begin our evaluation with a brief comparison of Livneh and SPEAR winter mean SWE and precipitation. We do this by averaging over the winter season, Oct-April, for the period of dataset overlap, 1921-2011. We find that SPEAR has a negative snow bias across much of the Mountain West, see Figure 1. In particular, regions characterized by high elevation often have SWE values over 100% higher in the Livneh dataset than SPEAR. This is not particularly surprising however, as resampling the 1/16° Livneh grid to the 1/2° grid for comparison with the coarse SPEAR data introduces bias as higher elevations have disproportionately more snow as compared with elevation (McCrary et al., 2022). Precipitation biases are consistently high across much of the Western US as seen in Figure 1 – these findings are consistent with Delworth et al. (2020).

However, despite these large absolute biases, we can still use SPEAR to quantify future snow droughts if it reasonably reproduces trends in SWE, temperature, and precipitation. To make these comparisons we leverage the distribution of the SPEAR large ensemble, allowing us to create a distribution of potential historical outcomes, to compare against the Livneh dataset.

##### 3.1.2 Evaluating Snow Drought Changes across the Historical Period

When examining historical changes, we find that SPEAR historical snow drought and temperature trends are already significant, based on a 95% confidence interval for the ensemble mean assuming an underlying normal distribution in changes. Changes in SWE across all 5 studied HUC2 regions, the Upper Colorado, Lower Colorado, Great Basin, Pacific Northwest, and California regions (abbreviated UC, LC, GB, PNW, and CA) show with ensemble means ranging from 26% (LC) to 53% (UC) increases in D2+ SD occurrence, as in Table 2. The Livneh dataset always falls within the ensemble spread (Table 2), although it is not always in the ensemble mean 95% CI. We present the distribution of D2+ SDs across the historical period (1980-2011) for SPEAR ensemble members, the SPEAR mean, and confidence interval, along with the Livneh observation in Figure 3. These results were consistent with findings in Huning and AghaKouchak (2020), who use 1980-2018 as their historical period — in fact, the 95% confidence interval for the SPEAR ensemble mean across 4 of the 5 regions contains the 28% benchmark for drought intensity increases found in Huning and AghaKouchak (2020), with only the UC interval exceeding the benchmark with a 30% lower bound on historical D2+ SD increases. While we were unable to use an identical historical period due to data constraints, the agreement helps to further validate the SPEAR ensemble. See supplemental section ?? and Figure ?? for an analysis of changes in precipitation and temperature across the historical period.

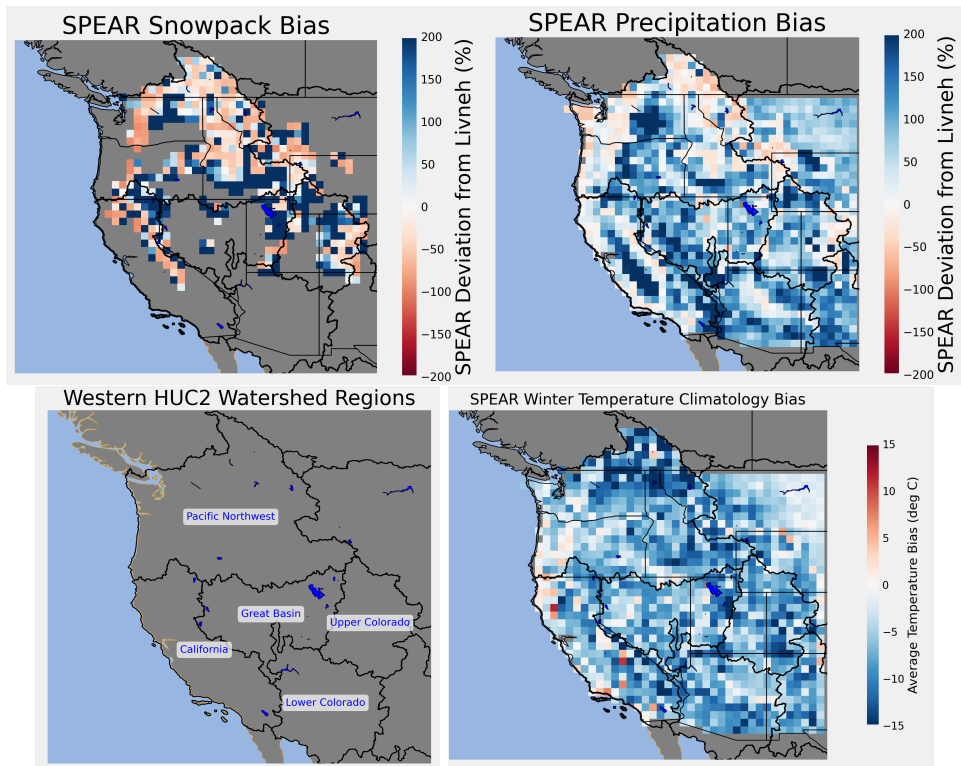


**Figure 1.** Clockwise from top left: SPEAR yearly (a) snowpack (%) and (b) precipitation (%) biases as compared to Livneh and (c) shows the 5 study HUC2 regions of interest.

Historical Changes in Snow Drought Frequency by Region (%)				
HUC2 Region	Livneh Increase	SPEAR Avg Increase	SPEAR Mean 95% CI	SPEAR Ensemble Range
Upper Colorado	4	53	[30, 77]	[-50, 236]
Lower Colorado	14	26	[13, 40]	[-39, 107]
Great Basin	45	48	[26, 70]	[-40, 225]
Pacific Northwest	-55	43	[16, 71]	[-68, 255]
California	9	46	[25, 67]	[-34, 192]

**Figure 2.** Summary table of Livneh and SPEAR average D2+ SD frequency changes for each of the 5 Western HUC2 regions. Changes are measured between the early (1930-1970) and late (1971-2011) historical periods. As SPEAR is a large ensemble we include a 95% confidence interval which assumes normally distributed changes, and a range of changes across the ensemble.

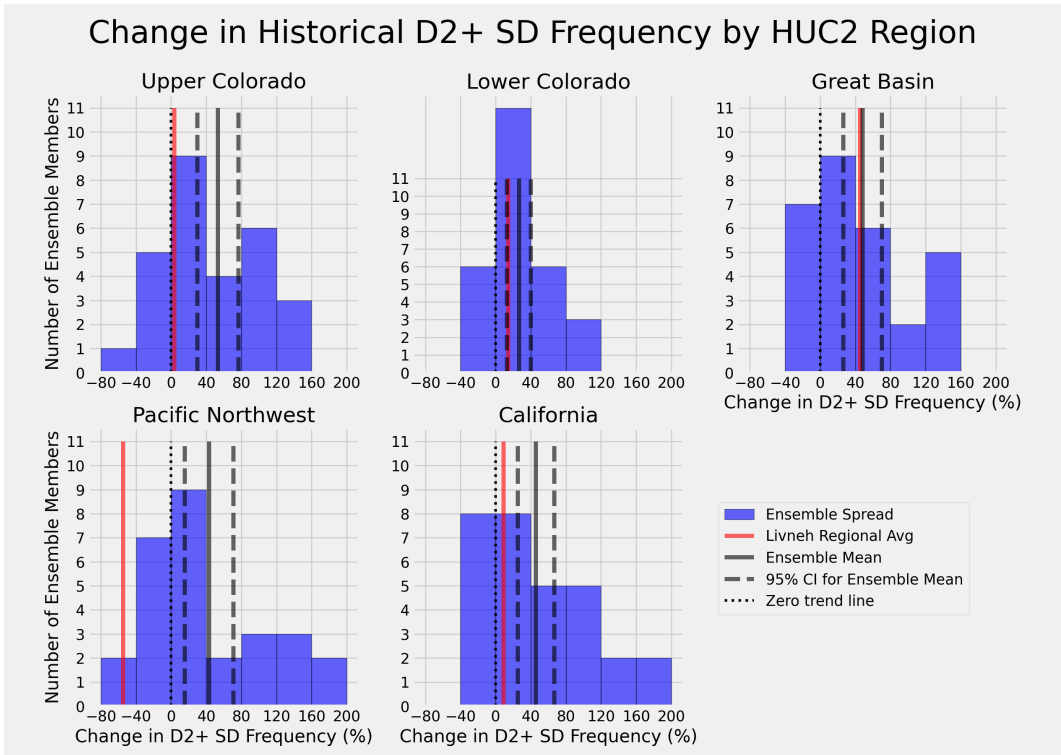


**Figure 3.** Comparison of SPEAR estimated D2+ SD increases across the historical to Livneh observed increases. The SPEAR distribution is given by the histogram in blue, with the red vertical line representing the observed change in the Livneh dataset. The solid and dashed gray lines represent the mean and 95% confidence interval for each regions' ensemble mean, while the dotted line represents the zero trend line. SPEAR estimates that all regions have experienced a significant increase in D2+ SDs over the historical period.

267            **3.2 Analyzing Snowpack into the 21<sup>st</sup> Century: Accelerating Loss**

268            We next shift our attention to projected changes in 21<sup>st</sup> century D2+ SD, focusing  
 269            first on changes in droughts classified directly with our ZSWE metric. We construct  
 270            our empirical CDF  $\hat{F}_{i,j}^k$  distributions from the historical period (1921-2011) and calculate  
 271            corresponding ZSWE scores for each winter month across the historically snowy west  
 272            2014-2100 for all 30 ensemble members. Projected changes in snowpack are dramatic,  
 273            with rapid increases in D2+ SD occurring at mid-century (Figure 4). Under SSP5-8.5  
 274            we find that towards the end of the century, all regions are projected to experience se-  
 275            vere drought, or more severe, during most months. Under SSP2-4.5, changes in snow drought  
 276            occurrence at the end of the century resemble snow drought conditions near mid-century  
 277            in the SSP5-8.5 ensemble. Thus, a higher forcing scenario is expected to accelerate SWE  
 278            decreases by several decades by the end of the century. Snow drought percentages for  
 279            all 18 study decades are shown in supplemental Figure ??.

280            Examining the distribution of D2+ SDs spatially in Figure 4, a pattern of regional  
 281            "hot-spots" emerge, where D2+ SD frequency is consistently higher in certain regions  
 282            beginning in 2030. For example the Washington Cascades and Colorado Rockies are pre-  
 283            dicted to experience more frequent snow drought occurrences across all decades than re-  
 284            gions in south-central Idaho and the California Sierra Nevada. We expected to see the  
 285            more southern basins have more dramatic increases in snow drought, such as the Col-  
 286            orado Rockies or California regions, as even low amounts of warming at southern lat-  
 287            itudes results in strong loss signals (Shrestha et al., 2021). We hypothesize that we are  
 288            looking over a narrow enough range of latitudes that the latitude signal is overshadowed  
 289            by regional variation, perhaps coming from elevation variability. Shrestha et al. (2021)  
 290            looked at basins ranging from the Yukon to Columbia river basins that have average win-  
 291            ter temperatures of -8°C to +4°C, finding that below -5°C to -6°C warming temperatures  
 292            didn't reduce snowpack. Our HUC2 regions had mean winter temperatures in histori-  
 293            cally snowy regions ranging from -5.1°C (UC) to 0.3°C (California), and so we expect  
 294            that any warming will produce decreases in snowpack, and corresponding increases in  
 295            D2+ SD occurrence.

296            While Figure 4 demonstrates the expected impacts of increasing greenhouse gases  
 297            over the next century, as captured by the ensemble mean, it does not indicate how in-  
 298            ternal climate variability, as captured in the ensemble spread, may exacerbate or alle-  
 299            viate the radiatively forced changes. As regions must be prepared for conditions less fa-  
 300            vorable than an ensemble mean, the SPEAR large ensemble allows us to quantify the  
 301            uncertainty of these ensemble mean changes that is attributable to internal variability.  
 302            By aggregating across grid cells and then looking at changes for individual ensemble mem-  
 303            bers as well as for the ensemble mean and 95%CI, we can visualize changes in the en-  
 304            semble's snow drought through time (Figure 5).

305            Figure 5 shows the percentage of months by decade which experience severe (D2+)  
 306            snow drought. We find that while ensemble members on average experience 5-12% of their  
 307            months as D2+ SDs in the historical period, under SSP5-8.5 this likelihood increases to  
 308            over 50% snow drought frequency by 2050. Under SSP2-4.5, the time-frame for 50% snow  
 309            drought occurrence increases to 2070. We note the SSP5-8.5 curve is initially flat un-  
 310            til 2000, where snow drought occurrence starts increasing and continues to grow unchecked;  
 311            under SSP2-4.5 the curve has a second inflection point at 2050, where the increase in snow  
 312            droughts flattens significantly.

313            **3.3 Temperature and Precipitation Controls on SWE**

314            As changes in SWE are primarily driven by changes in temperature and precipi-  
 315            tation climatology (McCrary et al., 2017; Harpold et al., 2017), we next examine changes  
 316            in SWE in the phase space spanned by temperature and precipitation. By aggregating

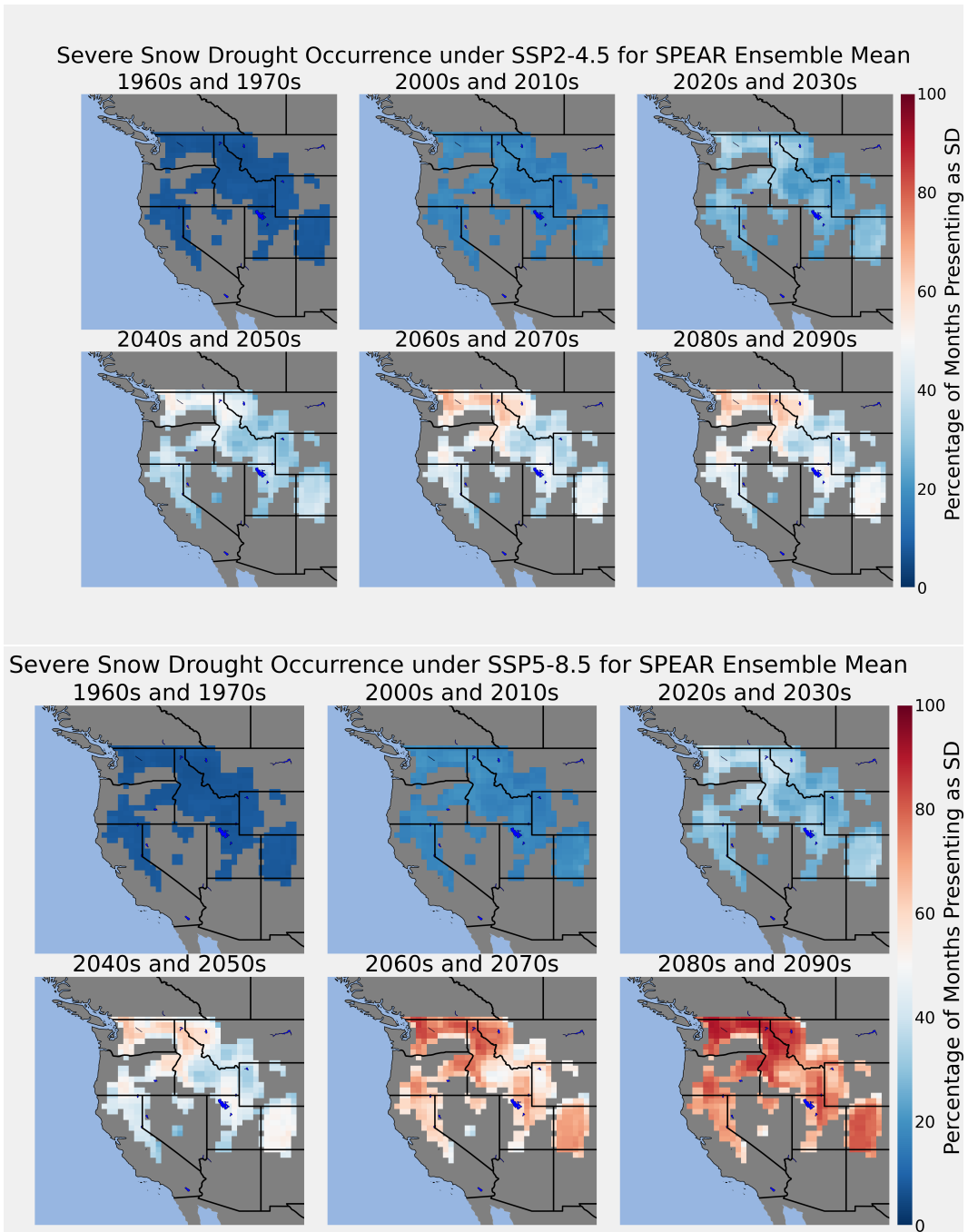


**Figure 4.** SPEAR snow drought changes highlighted from 1960-2100 under low (SSP2-4.5) and high (SSP5-8.5) emissions scenarios. The plots are masked to historically snowy regions which are colored by the percentage of winter months that the grid-cell experiences snow drought grouped every 2 decades. Historically snowy regions are characterized by having an average peak SWE of at least 20mm.

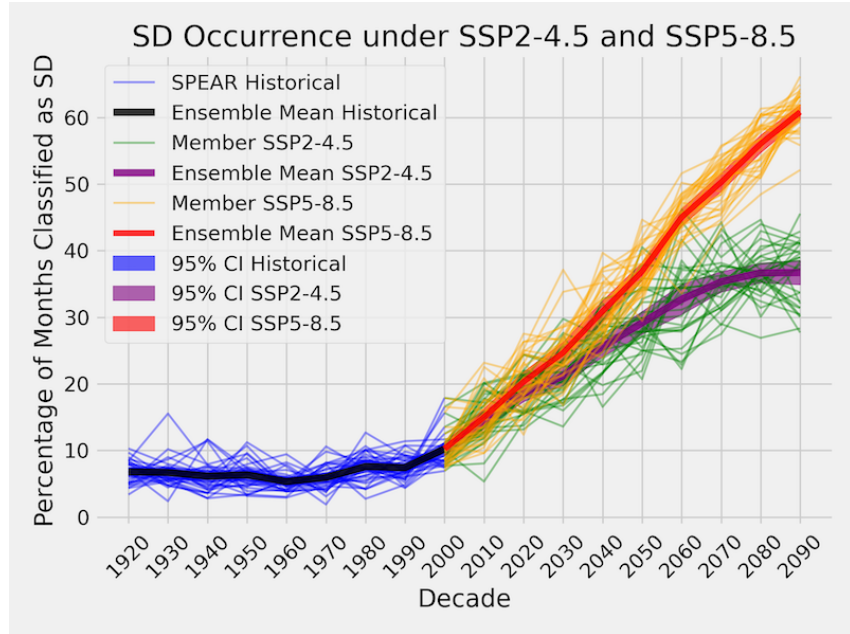


**Figure 5.** Decadal average of the number of SD months per grid cell. The green trend curves represent the ensemble mean averages for the historical and RCP 4.5 scenarios, while the orange curves depict the RCP 8.5 scenario. Ensemble mean and error is shaded darker.

over the entire historically snowy Western United States, we can determine how temperature and precipitation anomalies are driving the dramatic increase of droughts.

In Figure 6, each dot represents the average temperature and precipitation anomaly by decade and is colored according to the average ZSWE score. By definition, the average all-month historical (1921-2011) temperature and precipitation mean is  $(0, 0)$ . However, by breaking the century down by decade we can see variation within the 20<sup>th</sup> century.

As expected, points early in the historical period for the all month average cluster around zero temperature and precipitation deviation, and move as the underlying temperature and precipitation climatology shifts. In general we see very small changes in anomalies between decades before 2000. Beginning with the 2000s, the decadal averages for the all-month condition rapidly shift towards warmer and wetter conditions. For example, by 2050 under SSP5-8.5, the average temperature and precipitation are 1.50 and 0.25 standard deviations higher than the 20<sup>th</sup> century average, respectively. This corresponds to a dramatic warming and slight wetting across the WUS, and indicates that we expect the average month in 2050 to be warmer than 93% of months in the historical period for a given location. For SSP2-4.5, the values are 1.18 and 0.20, reflecting a still moderate increase in temperature and precipitation by mid-century, with the average month in 2050 being warmer than 88% of historical months.

To investigate how droughts specifically are changing, we average over just months which meet the D2+ criteria to see how the average drought month has changed (outlined in grey in Figure 6). We find that historical averages are both dry and warm with the average D2+ drought having a temperature and precipitation anomaly of 0.6 to 0.8 and -0.6 to -0.8, respectively, indicating historical snow droughts are primarily driven by a combination of both warm and dry conditions. This corresponds to a drought month on-average being both warmer and drier than 75% of months.

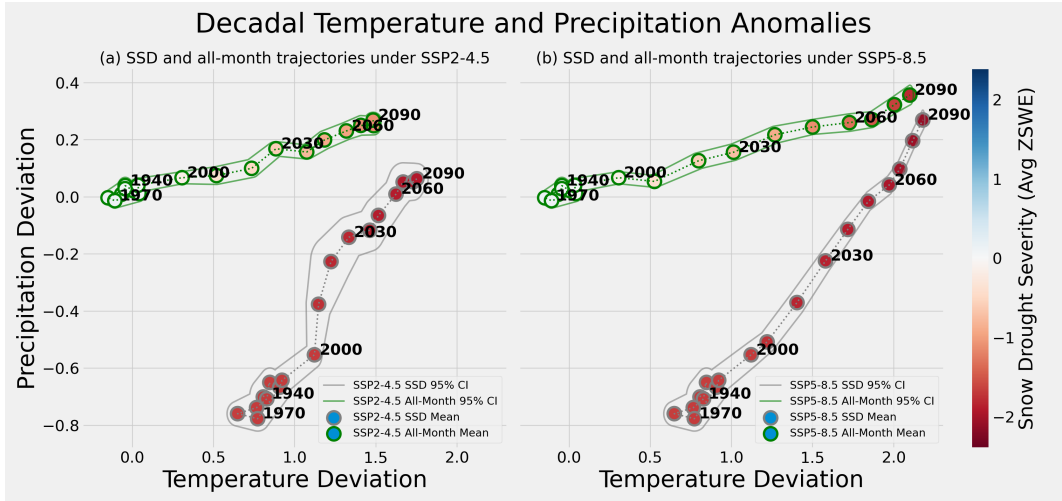


**Figure 6.** Temporal evolution of average temperature and precipitation anomalies with respect to the historical conditions (1921–2011). Each dot represents the average temperature and precipitation condition for historically snowy locations during winter (Oct–April) for a given decade either for all months and locations (outlined in green) or only for months classified as D2+ (outlined in gray). Each point is shaded by its average ZSWE score; thus because SSD months are subset to have a ZSWE of  $\geq -1.3$ , these points average conditions strictly less than -1.3. Both all-month and SSD-month points are surrounded by a contour which captures 95% of ensemble members. Panel (a) depicts these changes under SSP2-4.5 while (b) depicts changes under SSP5-8.5.

343 However, by 2050 the average drought has become both warmer *and* wetter; under  
 344 SSP5-8.5 the temperature deviation increases to 1.84 and the precipitation deviation  
 345 increases to -0.015, meaning that it no longer takes any deviation from normal historical  
 346 precipitation to produce a drought, and D2+ snow drought conditions are driven  
 347 by the temperature average which is warmer than 97% of historical conditions. Under  
 348 SSP2-4.5 the mean temperature and precipitation deviations are 1.51 and -0.065, respec-  
 349 tively. By 2090, the average drought month has a temperature deviation of 2.18 and pre-  
 350 cipitation deviation of 0.27, very close to the all-month anomalies of 2.10 and 0.36 for  
 351 temperature and precipitation respectively. Note that the average monthly temperature  
 352 for both D2+ and all-month averages are in the 98th percentile of historical conditions,  
 353 indicating not only that future winter conditions will on average be extremely warm, but  
 354 that there is no longer a statistically significant difference between average conditions  
 355 for all months, and drought months alone. Examining the ZSWE scores for 2090 under  
 356 SSP5-8.5 confirms the convergence, with the average all-month ZSWE being -1.79 and  
 357 the average D2+ month having a ZSWE of -2.10. This corresponds to the all-month av-  
 358 erage falling in the D3, or extreme drought category, while the average drought is ex-  
 359 pected to be exceptional, or D4. Under SSP2-4.5, conditions do not become quite as ex-  
 360 treme, with average all-month conditions by 2090 reaching 1.48 for temperature, 0.27  
 361 for precipitation, and -1.10 ZSWE. We note that although the gap to the D2+ condi-  
 362 tion narrows (1.75, 0.064, and -1.91 for T, P, and ZSWE), it is far less extreme than un-  
 363 der SSP5-8.5; the average month is only given a D1 snow drought classification. The con-  
 364 vergence of the all-month and D2+ temperature and precipitation anomalies, particu-  
 365 larly under SSP5-8.5 emphasize that severe snow droughts will require increasingly smaller  
 366 deviations from normal conditions to produce, underscoring that snow droughts will be-  
 367 come the dominant regime in the WUS by the end of the 21<sup>st</sup> century.

### 368      3.4 Timeline for Snow Free Conditions

#### 369      3.4.1 *Transition to No-Snow Regime*

370      By examining how the distribution of no-snow transitions changes as a function of  
 371      the area threshold,  $\mathcal{A}$ , we can understand the severity of snowpack loss each region is  
 372      expected to experience by 2100. Figure 7 shows the distribution of the transition to no  
 373      snow regimes for 3 different area thresholds,  $\mathcal{A}$ : 50%, 75%, and 90%, for the historically  
 374      snowy HUC2 regions. Note that by construction, an individual ensemble member's trans-  
 375      sition year always occurs later for higher  $\mathcal{A}$ , however the distributions themselves over-  
 376      lap, indicating large variability in the severity of conditions especially later this century.

377      For  $\mathcal{A} = 0.5$ , we find that the mean transition time for all regions is 2059 for SSP2-  
 378      4.5 and 2040 for SSP5-8.5. However, across regions transition times varied from as early  
 379      as 2025 (CA) to 2088 (UC) for SSP2-4.5 and 2018 (CA) to 2056 (UC) for SSP5-8.5 for  
 380      the 291 out of 300 regions that transitioned before 2100. Across all regions, the snow-  
 381      free transition distribution is shifted later for SSP2-4.5 scenario when compared with SSP5-  
 382      8.5, with more similar distributions between scenarios occurring in regions which ex-  
 383      perience a no-snow transition earlier, such as California. The overlap highlights that while  
 384      a lower emission scenario improves the probability that a snow-free transition occurs later  
 385      in the 21st century than would be expected under the higher emission scenario, it does  
 386      not guarantee that this happens due to internal climate variability.

387      Another notable feature of Figure 7 is the distribution within each region of the  
 388      30-ensemble member transition times generated by internal climate variability. We find  
 389      that in some realizations and regions the earliest transition occurs over 15 years earlier  
 390      than the median transition for many regions. For example, in the Lower Colorado re-  
 391      gion, the first ensemble member transitions in 2069 while the mean transition time of  
 392      the ensemble members isn't until 2086. Thus, while the LC is not likely to see these ex-  
 393      treme conditions until the 2080s according to SPEAR, their hydrological infrastructure,  
 394      snow tourism economies, and fire response must be prepared significantly earlier to face  
 395      these conditions. The ensemble spread also indicates that for most regions, the earliest  
 396      transition under the SSP2-4.5 scenario is nearly as early as that of the higher emission  
 397      scenario. For example, in the Pacific Northwest a quarter of the SSP2-4.5 realizations  
 398      occurred before the latter half of the SSP5-8.5 realizations. This suggests emission re-  
 399      ductions, while likely to improve the odds that a no-snow transition occurs later in the  
 400      century, is not a guarantee, particularly for regions where the transition is projected to  
 401      occur before 2050.

402      Under SSP2-4.5 the distribution of when the transition occurs in Figure 7 is more  
 403      spread out and is centered later in comparison to the SSP5-8.5 distribution. This is con-  
 404      sistent with our expectation that more rapid warming under SSP5-8.5 will accelerate the  
 405      timeline associated with a transition to low snow, the compressed timeline is simply a  
 406      byproduct of this effect. In other words, temperature and precipitation changes are hap-  
 407      pening more slowly in SSP2-4.5 which leads to internal climate variability being a more  
 408      important factor in determining no-snow transition times, as in SSP5-8.5 the accelerated  
 409      radiative forcing is the dominant effect.

#### 410      3.4.2 *Assessing the Likelihood of a Snow Free West by 2100*

411      To assess the probability that a region becomes snow free over the next century,  
 412      we examine the fraction of ensemble members that transition to no-snow before 2100.  
 413      We model the likelihood of the transition by the maximum likelihood estimator (MLE),  
 414      or fraction of ensemble members that hit the transition threshold by 2100, and display  
 415      these values in Table 8. By further splitting across the low and high emission scenarios,  
 416      we can model how the risk also changes as a function of the radiative forcing scenario.  
 417      In Table 8b, we see that under SSP5-8.5,  $\mathcal{A} = 0.75$  is guaranteed by 2100 across all re-  
 418      gions. The highest threshold,  $\mathcal{A} = 0.9$  is guaranteed only for California, while uncer-

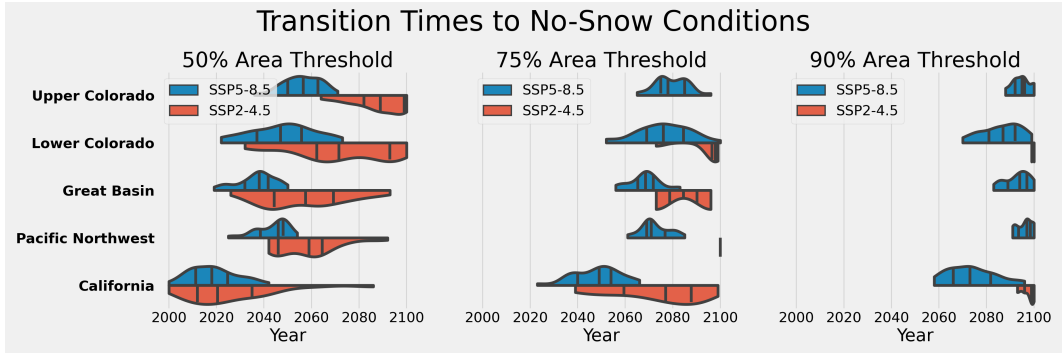


**Figure 7.** Distribution of SPEAR-simulated transition times to no snow regimes, or  $\mathcal{T}$ , by Western HUC2 region, split between SSP5-8.5 and SSP2-4.5 scenarios. The 3 subplots represent the different thresholds  $\mathcal{A}$ . Meeting a higher threshold corresponds with an increased proportion of the region experiencing perennial no-snow conditions, and implies more severe conditions.

tainty remains for the other 4 HUC2s. Conditions by 2100 are much less severe under SSP2-4.5, with only  $\mathcal{A} = 0.5$  likely or certain for all regions, while for  $\mathcal{A} = 0.75$ , only California is very likely to transition to a low snow regime; the other regions have low probability of doing so. For  $\mathcal{A} = 0.9$  it is unlikely that any region will have transitioned by 2100 under SSP2-4.5.

When we compare the order of how likely regions are to transition to no-snow conditions under any scenario to the average mean historical temperature of historically snowy areas, we find a striking similarity. Using SSP5-8.5 with a 90% area threshold as our reference column in Figure 8, and noting their mean winter temperatures we order from least to most likely as UC ( $-5.1^{\circ}\text{C}$ , 30%), PNW ( $-3.9^{\circ}\text{C}$ , 53%), GB ( $-2.4^{\circ}\text{C}$ , 70%), LC ( $-0.7^{\circ}\text{C}$ , 83%), and CA ( $0.3^{\circ}\text{C}$ , 100%); the orderings are identical. This finding emphasizes the role mean winter temperature plays in dictating a regions no-snow transition probability. Like Shrestha et al. (2021) we find that warming any region with a winter average of  $>5^{\circ}\text{C}$ , negatively impacts snowpack. Strikingly, under either scenario, we expect the majority of the historically snowy WUS to have less than 10% of its historical snowpack by 2100, even under a low to moderate SSP2-4.5 emissions scenario. Under a high emissions scenario, we find that it's likely that 4 of the 5 Western watersheds are expected to cross our highest threshold of 90% snow-free by 2100, with the Upper Colorado being the exception with only a 30% chance. While these numbers are shocking, it's important to consider how an understanding area and total snow volume differ. As snowpack declines have been dominated by losses at lower elevations that are closer to the freezing point, and we conclude that the extreme loss of area predicted by SPEAR may overestimate the amount of total winter water storage lost since the higher elevations typically store the most snowpack (Mote et al., 2005; Minder, 2009). Therefore we expect the area-based no-snow transition to over-predict the hydrological impact of warming.

#### 4 Remarks

Widespread increases in D2+ snow droughts have already been observed in the historical period, according to SPEAR, which estimates that across the WUS D2+ SD frequency has increased by 43%, with an average 95% confidence interval of 22 to 65%. These findings are slightly higher, although still consistent with Huning and AghaKouchak (2020) whose slightly different time period found a 28% increase in D2+ SD frequency for the WUS over 1980-2018. SPEAR predicts even more dramatic changes heading into the 21<sup>st</sup>

## Probability of No-Snow Transition by 2100

Region	SSP2-4.5			SSP5-8.5		
	50%	75%	90%	50%	75%	90%
Upper Colorado	83	0	0	100	97	30
Lower Colorado	87	23	7	100	100	83
Great Basin	100	7	0	100	100	70
Pacific Northwest	100	3	0	100	100	53
California	100	93	17	100	100	100

**Figure 8.** Probability of a snow free transition occurring before 2100 at the 3 thresholds  $\mathcal{A}$  based on the fraction of ensemble members who transition to a no-snow regime by 2100. We show the probabilities by area threshold, 50%, 75%, and 90%, across SSP2-4.5 and SSP5-8.5 for the historically snowy portions of each of the 5 Western HUC2 regions.

century, classifying over 35% of winter months as snow droughts under RCP2-4.5 and 60% under RCP5-8.5 by 2100, compared with a normalized 9.6% across the historical period. These changes were found to be primarily driven by increasing temperatures, which on average exceeded the 93<sup>rd</sup> and 97<sup>th</sup> percentile (2 standard deviations) of historical temperature records by 2100 under RCP2-4.5 and RCP4-8.5, respectively. We also found that across all regions, the transition to a no-snow regime, where over 90% of the historically snowy region had on average less than 10% of the April historical maximum, was more likely than not in 4 out of the 5 HUC2s studied under RCP5-8.5, the UC region being the exception. Under RCP2-4.5, only the 50% threshold was exceedingly likely for all regions, emphasizing the role that emissions this century will play in determining D2+ SD frequency.

Similar to Shrestha et al. (2021), who found a strong correlation between decreasing latitude, as a proxy for temperature, and decreased snowpack, with the probability of a no-snow transition much more likely for regions which have higher average winter temperatures in historically snowy locations. In particular, the Lower Colorado and California Regions, which are the most Southern, had the highest probabilities of reaching no-snow conditions across both emissions scenarios and all area threshold values, and similarly had winter temperatures averaging near 0°C. The Pacific Northwest and Upper Colorado, the coldest regions on average, typically had the smallest transition probabilities. While using a GCM allows us to examine multiple realizations of the climate to derive these probabilities, it is inherently limited by the model assumption constraints. In particular, the large resolution of a 1/2° global climate model is unable to resolve complex mountain topography and can result in significant warm biases which predicts less snow at elevation, as shown by Matiu and Hanzer (2022). We expect that this may make

476 SPEAR snowpack estimates particularly sensitive to warming, and therefore likely to over-  
 477 estimate increases in snow drought.

478 Here, we've assessed changes in snow drought frequency, focusing on how the un-  
 479 derlying climatology is expected to change, alongside broader implications for the WUS  
 480 by modeling the distribution of expected no-snow transition times. This study has im-  
 481 pacts for Western hydrology, alongside snow tourism which is expected to see losses of  
 482 50% of the ski season by 2050 and 80% by 2090 (Wobus et al., 2017). Several avenues  
 483 for future research include: examining snow drought frequency changes over smaller re-  
 484 gions, such as looking at HUC4 regions to tease out which sub-regions are most vulner-  
 485 able, which would allow us to further examine latitude and elevation dependence. Es-  
 486 timating total SWE losses and melt timing across each region would allow us to better  
 487 estimate the impacts of snow droughts on the West's hydrological system. The impacts  
 488 of future snow droughts will be felt across the entire country, either directly from the hy-  
 489 drological or tourism resources that consistent snowpack provides, or indirectly through  
 490 loss of agricultural output from summer water shortages or drifting wildfire smoke.

#### 491 Acknowledgments

492 Many thanks to Sarah Kapnick for helping to inspire this project. We would also like  
 493 to thank the NOAA Hollings Scholarship Program for funding this research.

#### 494 References

- Barnett, T. P., Adam, J. C., & Lettenmaier, D. P. (2005, November). Potential  
 495 impacts of a warming climate on water availability in snow-dominated re-  
 496 gions. *Nature*, 438(7066), 303–309. Retrieved 2022-07-26, from <https://www.nature.com/articles/nature04141> (Number: 7066 Publisher: Nature  
 497 Publishing Group) doi: 10.1038/nature04141
- Delworth, T. L., Cooke, W. F., Adcroft, A., Bushuk, M., Chen, J.-H., Dunne,  
 500 K. A., ... Zhao, M. (2020). Spear: The next generation gfdl modeling  
 501 system for seasonal to multidecadal prediction and projection. *Journal of  
 502 Advances in Modeling Earth Systems*, 12(3), e2019MS001895. Retrieved  
 503 from <https://agupubs.onlinelibrary.wiley.com/doi/abs/10.1029/2019MS001895> (e2019MS001895 2019MS001895) doi: <https://doi.org/10.1029/2019MS001895>
- Deser, C., Lehner, F., Rodgers, K. B., Ault, T., Delworth, T. L., DiNezio, P. N.,  
 507 ... Ting, M. (n.d.). Insights from earth system model initial-condition large  
 508 ensembles and future prospects. , 10(4), 277–286. Retrieved 2022-08-31, from  
 509 <https://www.nature.com/articles/s41558-020-0731-2> (Number: 4 Publisher:  
 510 Nature Publishing Group) doi: 10.1038/s41558-020-0731-2
- Gergel, D. R., Nijssen, B., Abatzoglou, J. T., Lettenmaier, D. P., & Stumbaugh,  
 512 M. R. (n.d.). Effects of climate change on snowpack and fire potential in the  
 513 western USA. , 141(2), 287–299. Retrieved from <https://doi.org/10.1007/s10584-017-1899-y> doi: 10.1007/s10584-017-1899-y
- Harpold, A., Dettinger, M., & Rajagopal, S. (2017, 02). Defining snow drought and  
 516 why it matters. *Eos Transactions American Geophysical Union*. doi: 10.1029/  
 517 2017EO068775
- Huning, L. S., & AghaKouchak, A. (2020). Global snow drought hot spots and  
 519 characteristics. *Proceedings of the National Academy of Sciences*, 117(33),  
 520 19753–19759. Retrieved from <https://www.pnas.org/doi/abs/10.1073/pnas.1915921117> doi: 10.1073/pnas.1915921117
- Kim, R. S., Kumar, S., Vuyovich, C., Houser, P., Lundquist, J., Mudryk, L.,  
 523 ... Wang, S. (2021). Snow ensemble uncertainty project (seup): quan-  
 524 tification of snow water equivalent uncertainty across north america via  
 525 ensemble land surface modeling. *The Cryosphere*, 15(2), 771–791. Re-

- trieved from <https://tc.copernicus.org/articles/15/771/2021/> doi: 10.5194/tc-15-771-2021
- Livneh, B., Rosenberg, E. A., Lin, C., Nijssen, B., Mishra, V., Andreadis, K. M., ... Lettenmaier, D. P. (2013). A long-term hydrologically based dataset of land surface fluxes and states for the conterminous united states: Update and extensions. *Journal of Climate*, 26(23), 9384 - 9392. Retrieved from <https://journals.ametsoc.org/view/journals/clim/26/23/jcli-d-12-00508.1.xml> doi: 10.1175/JCLI-D-12-00508.1
- Matiu, M., & Hanzer, F. (2022). Bias adjustment and downscaling of snow cover fraction projections from regional climate models using remote sensing for the european alps. *Hydrology and Earth System Sciences*, 26(12), 3037–3054. Retrieved from <https://hess.copernicus.org/articles/26/3037/2022/> doi: 10.5194/hess-26-3037-2022
- McCrory, R. R., McGinnis, S., & Mearns, L. O. (2017). Evaluation of snow water equivalent in narccap simulations, including measures of observational uncertainty. *Journal of Hydrometeorology*, 18(9), 2425 - 2452. Retrieved from [https://journals.ametsoc.org/view/journals/hydr/18/9/jhm-d-16-0264\\_1.xml](https://journals.ametsoc.org/view/journals/hydr/18/9/jhm-d-16-0264_1.xml) doi: 10.1175/JHM-D-16-0264.1
- McCrory, R. R., Mearns, L. O., Hughes, M., Biner, S., & Bukovsky, M. S. (2022, February). Projections of North American snow from NA-CORDEX and their uncertainties, with a focus on model resolution. *Climatic Change*, 170(3), 1-25. Retrieved from [https://ideas.repec.org/a/spr/climat/v170y2022i3d10.1007\\_s10584-021-03294-8.html](https://ideas.repec.org/a/spr/climat/v170y2022i3d10.1007_s10584-021-03294-8.html) doi: 10.1007/s10584-021-03294-8
- Minder, J. R. (2009). The sensitivity of mountain snowpack accumulation to climate warming. *Journal of Climate*, 23, 2634 - 2650.
- Mote, P. W., Hamlet, A. F., Clark, M. P., & Lettenmaier, D. P. (2005). Declining mountain snowpack in western north america\*. *Bulletin of the American Meteorological Society*, 86(1), 39 - 50. Retrieved from <https://journals.ametsoc.org/view/journals/bams/86/1/bams-86-1-39.xml> doi: 10.1175/BAMS-86-1-39
- Shrestha, R. R., Bonsal, B. R., Bonnyman, J. M., Cannon, A. J., & Najafi, M. R. (2021). Heterogeneous snowpack response and snow drought occurrence across river basins of northwestern north america under 1.0 °c to 4.0 °c global warming. *Climatic Change*, 164(3), 40.
- Suurila-Woodburn, E. R., Rhoades, A. M., Hatchett, B. J., Huning, L. S., Szinai, J., Tague, C., ... Kaatz, L. (2021). A low-to-no snow future and its impacts on water resources in the western united states. *Nature Reviews Earth & Environment*, 2(11), 800–819. Retrieved from <https://doi.org/10.1038/s43017-021-00219-y> doi: 10.1038/s43017-021-00219-y
- Svoboda, M., LeComte, D., Hayes, M., Heim, R., Gleason, K., Angel, J., ... Stephens, S. (2002). The drought monitor. *Bulletin of the American Meteorological Society*, 83(8), 1181 - 1190. Retrieved from [https://journals.ametsoc.org/view/journals/bams/83/8/1520-0477-83\\_8\\_1181.xml](https://journals.ametsoc.org/view/journals/bams/83/8/1520-0477-83_8_1181.xml) doi: 10.1175/1520-0477-83.8.1181
- Trujillo, E., Molotch, N. P., Goulden, M. L., Kelly, A. E., & Bales, R. C. (n.d.). Elevation-dependent influence of snow accumulation on forest greening. , 5(10), 705–709. Retrieved 2022-07-26, from <https://www.nature.com/articles/ngeo1571> (Number: 10 Publisher: Nature Publishing Group) doi: 10.1038/ngeo1571
- Wobus, C., Small, E. E., Hosterman, H., Mills, D., Stein, J., Rissing, M., ... Martinich, J. (2017). Projected climate change impacts on skiing and snowmobiling: A case study of the united states. *Global Environmental Change*, 45, 1-14. Retrieved from <https://www.sciencedirect.com/science/article/pii/S0959378016305556> doi: <https://doi.org/10.1016/j.gloenvcha.2017.04.006>
- Wrzesien, M. L., Pavelsky, T. M., Durand, M. T., Dozier, J., & Lundquist, J. D.

582 (2019). Characterizing biases in mountain snow accumulation from global data  
583 sets. *Water Resources Research*, 55(11), 9873-9891. Retrieved from <https://agupubs.onlinelibrary.wiley.com/doi/abs/10.1029/2019WR025350> doi:  
584 <https://doi.org/10.1029/2019WR025350>